Supplement of Atmos. Chem. Phys., 16, 6511–6535, 2016
http://www.atmos-chem-phys.net/16/6511/2016/
doi:10.5194/acp-16-6511-2016-supplement

Atmospheric Chemistry and Physics
Open Access

Supplement of

Understanding the optical properties of ambient sub- and supermicron particulate matter: results from the CARES 2010 field study in northern California

Christopher D. Cappa et al.

Correspondence to: Christopher D. Cappa (cdcappa@ucdavis.edu)

Table S1. Summary of abbreviations and symbols used in this work.

Symbol	Definition
PCA_{NOx}	Average photochemical age of the air mass
PCA_{HC}	Average photochemical age of the air mass
PM_1	Particulate matter with aerodynamic diameter < 1 µm
PM_{10}	Particulate matter with aerodynamic diameter < 10 µm
$\mathrm{PM}_{\mathrm{super}}$	Particulate matter with aerodynamic diameter between 1 and 10 µm
$b_{\mathrm{sca,super}}$	Scattering attributed to particles between 1 and 10 µm
$b_{\mathrm{abs,super}}$	Absorption attributed to particles between 1 and 10 µm
$f_{\mathrm{sca,PM1}}$	Fraction of scattering from particles < 1 µm diameter (submicron)
$f_{\mathrm{abs,PM1}}$	Fraction of absorbing from particles < 1 µm diameter (submicron)
$f_{\mathrm{sca,super}}$	Fraction of scattering from particles between 1 and 10 µm diameter
$f_{\mathrm{abs,super}}$	Fraction of absorbing from particles between 1 and 10 µm diameter
$AAE_{\lambda1,\lambda2}$	Absorbing Ångstrom exponent from λ1 and λ2
AAE_{PM1}	Absorption Ångstrom exponent for particles < 1 µm diameter (submicron)
AAE_{PM10}	Absorption Ångstrom exponent for particles < 10 µm diameter
$\Delta AAE_{10\text{-}1}$	Absorption Ångstrom exponent for particles from 1 to 10 µm diameter
$\Delta AAE_{\mathrm{amb\text{-}TD}}$	Difference in AAE between ambient and thermodenuded states
$SAE_{\lambda1,\lambda2}$	Scattering Ångstrom exponent from a given wavelength pair (λ1 and λ2)
SAE_{PM1}	Scattering Ångstrom exponent for particles < 1 µm diameter (submicron)
SAE_{PM10}	Scattering Ångstrom exponent for particles < 10 µm diameter
$\Delta SAE_{10\text{-}1}$	Difference in scattering Ångstrom exponent for particles from 1 to 10 µm diameter
EAE_{PM10}	Extinction Ångstrom exponent for particles < 10 µm diamete
EAE_{PM10}-50	EAE_{PM10} value where $f_{\mathrm{sca,PM1}} = 0.5$
SSA	Single scatter albedo – fraction of extinction due to scattering
f_{bsca}	Fraction of light that is backscattered
g_{sca}	Asymmetry parameter
$f_{\mathrm{ext,TD}}$	Fraction of extinction remaining in the thermodenuder
γ_{RH}	Hygroscopicity
$\Delta\gamma_{\mathrm{RH}}$	Difference in hygroscopicity between undenuded and denuded
MAC_{PM1}	Mass absorption coefficient for particles < 1 µm diameter
MAC_{PM10}	Mass absorption coefficient for particles < 10 µm diameter
MAC_{super}	Mass absorption coefficient for particles from 1 to 10 µm diameter
MSC_{PM1}	Mass scattering coefficient for particles < 1 µm diameter
MSC_{PM10}	Mass scattering coefficient for particles < 10 µm diameter
MSC_{super}	Mass scattering coefficient for particles from 1 to 10 µm diameter
E_{abs}	Absorption enhancement
AOD	Aerosol Optical Depth
FMF	Fine mode fraction of extinction

Table S2. Results from linear fitting of SAE_{PM10} versus $f_{sca,PM1}$.

Wavelength Pair SAE_{PM10}	Wavelength $f_{sca,PM1}$ (nm)	Slope*	Intercept#
450-550	450	2.65	-0.34
450-550	550	2.69	-0.05
450-550	700	2.81	0.27
450-700	450	2.63	-0.41
450-700	550	2.70	-0.14
450-700	700	2.92	0.15
550-700	450	2.62	-0.47
550-700	550	2.71	-0.21
550-700	700	3.01	0.05
	T1		
450-550	450	2.62	-0.24
450-550	550	2.66	-0.06
450-550	700	2.76	0.40
450-700	450	2.69	-0.42
450-700	550	2.76	-0.14
450-700	700	2.97	0.18
550-700	450	2.77	-0.59
550-700	550	2.85	-0.31
550-700	700	3.15	-0.02
550-700	700	3.01	0.05

* The fit uncertainties were typically < 0.02, which is much smaller than the experimental uncertainty.

The fit uncertainties were typically < 0.01, which is much smaller than the experimental uncertainty.

Table S3. Summary of the EAE_{PM10}-50 values dependence on the wavelength pairs used. See Figure S6 for the relevant observations.

EAE_{PM10} Wavelength Pair (nm)	$f_{ext,PM1}$ Wavelength (nm)	EAE_{PM10}-50
450,550	450	0.92
450,550	550	1.15
450,550	700	1.42
450,700	450	0.85
450,700	550	1.09
450,700	700	1.37
550,700	450	0.79
550,700	550	1.03
550,700	700	1.32

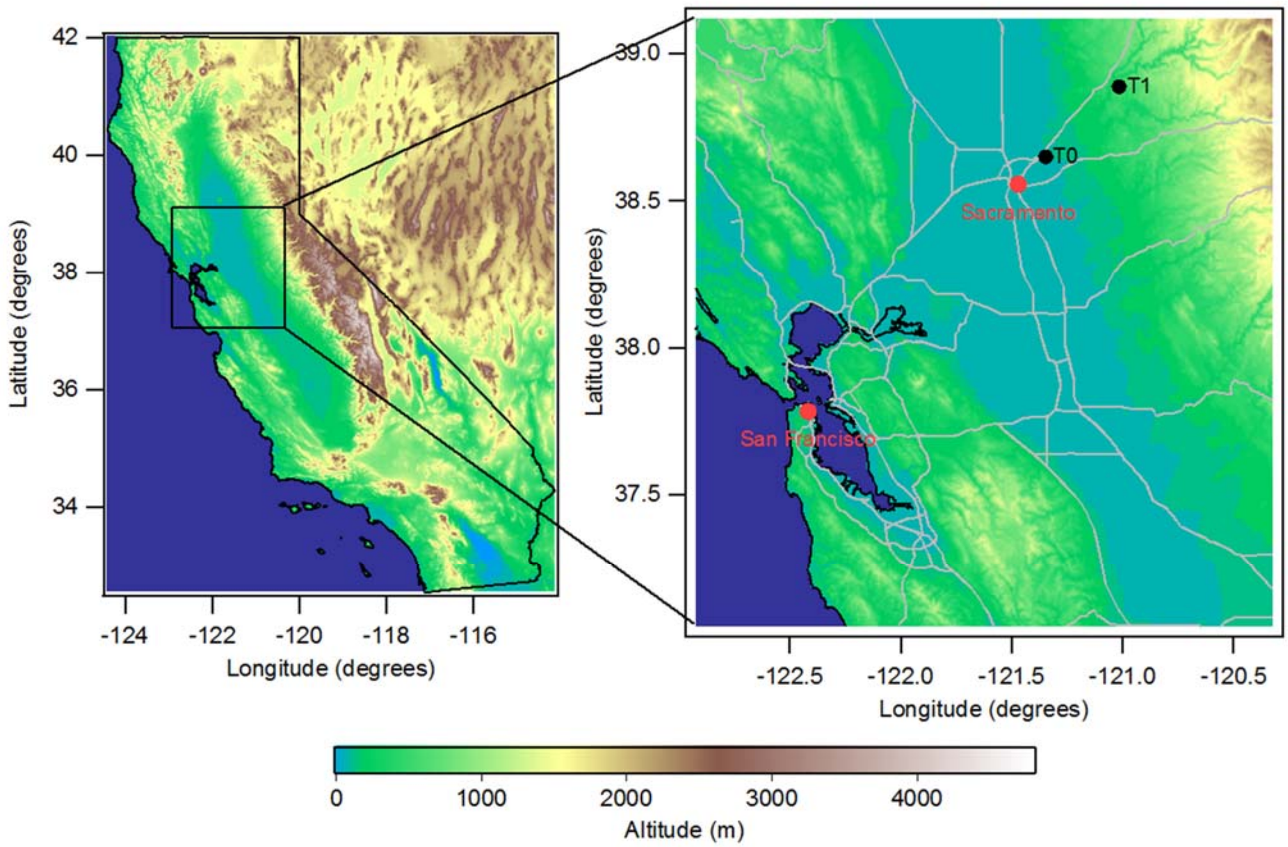

Figure S1. (left) A map of California, showing the general measurement location. (right) A closer-up view of the two observational sites, T0 near Sacramento, CA and T1 near Cool, CA. The gray lines show the main interstate and highway network. Dark blue areas indicate water.

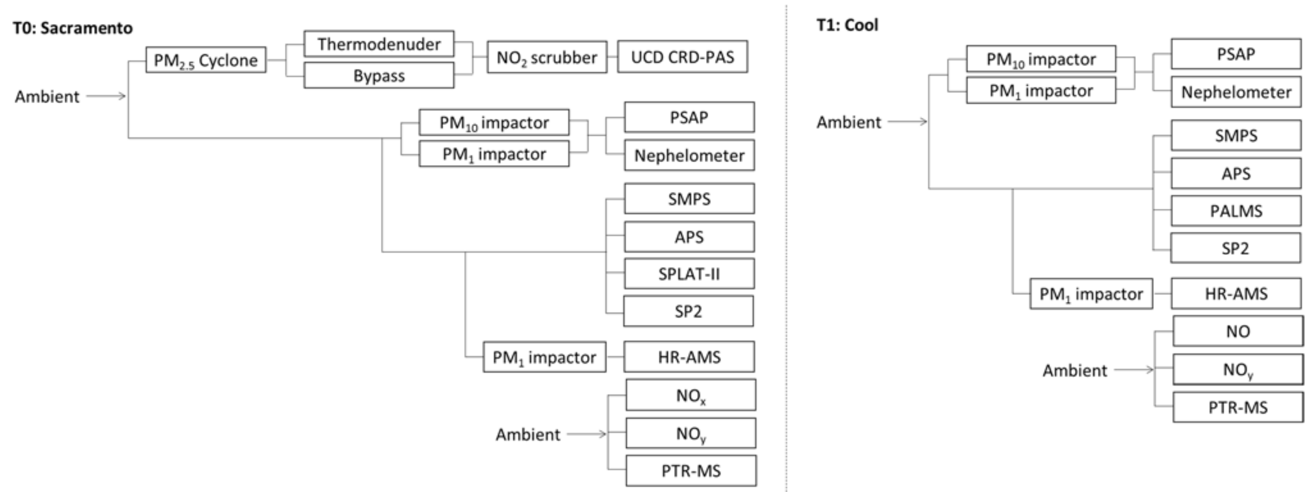

Figure S2. Schematic of the sampling scheme during CARES for the (left) T0 site in Sacramento and (right) T1 site in Cool.

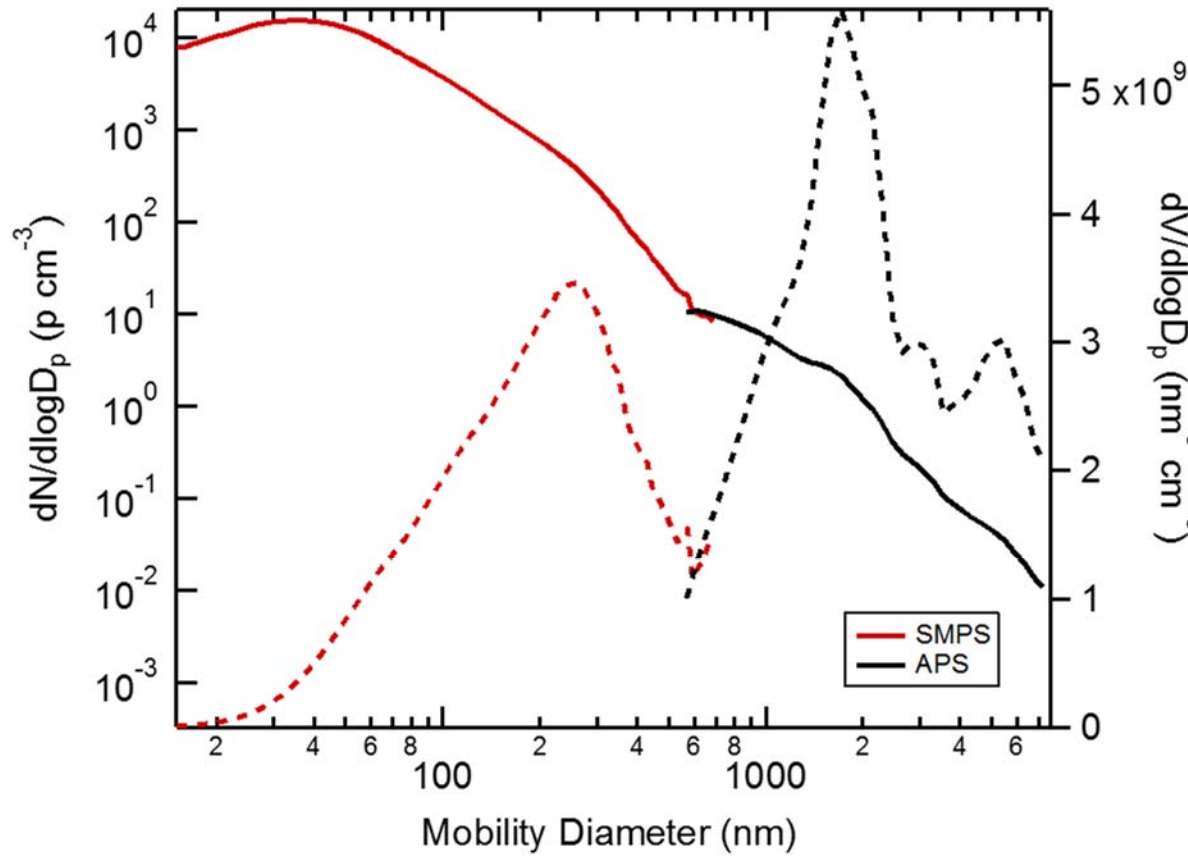

Figure S3. Merged campaign-average mobility-equivalent size distribution for the T0 site showing the measurements made using the SMPS (red) and APS (black). The APS aerodynamic diameters were adjusted to mobility-equivalent diameters assuming a material density of 2.0 g cm^{-3}. The number-weighted distribution is shown as solid lines and the volume-weighted size distribution as dashed lines.

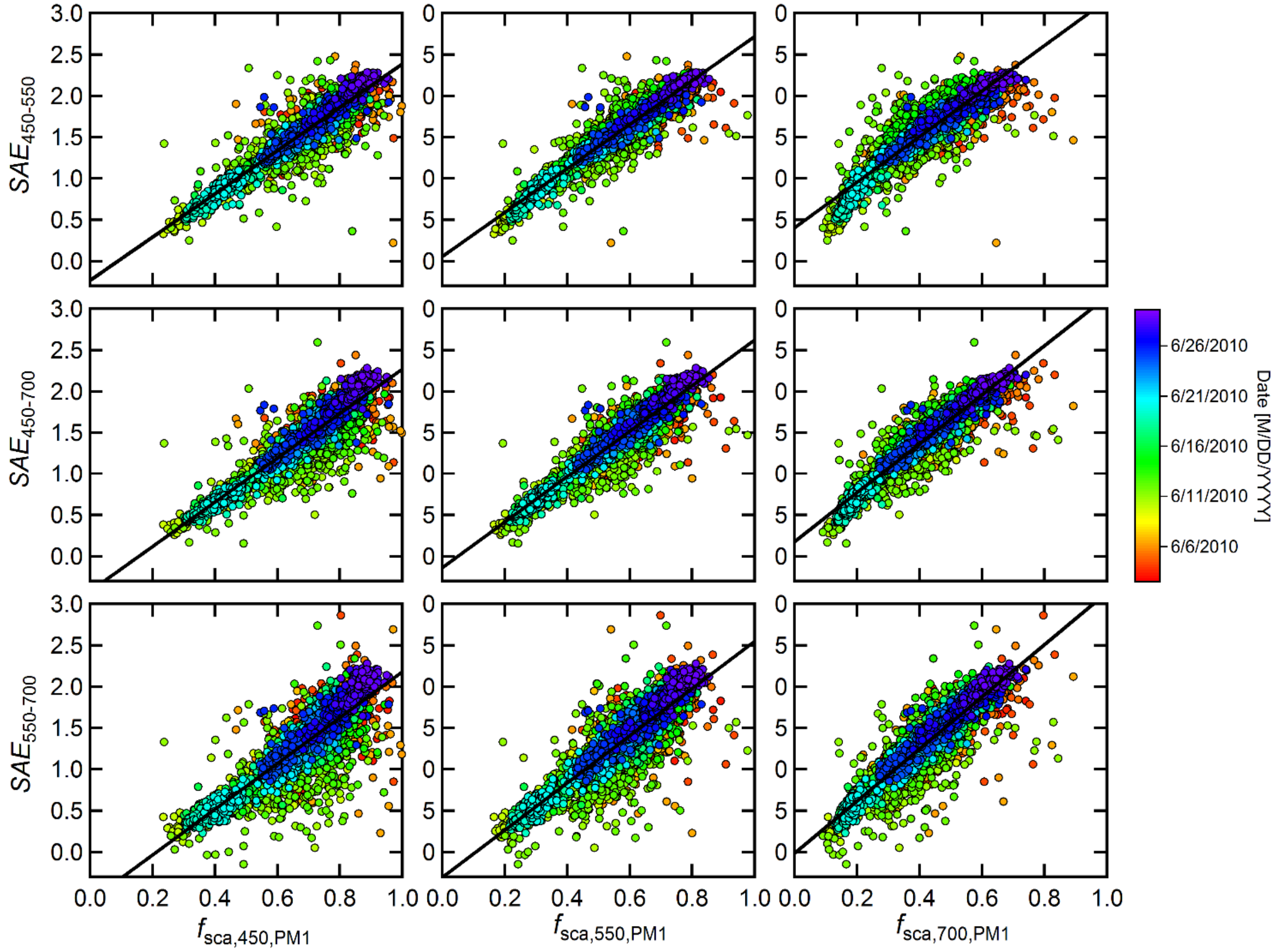

Figure S4. The relationship between the scattering Ångstrom exponent for PM_{10} for different wavelength pairs and the PM_1/PM_{10} scattering ratio ($f_{sca,PM1}$) at different wavelengths for the T0 site. The points are colored according to time during the campaign. Slope and intercept values from the linear fits (black lines) are reported in Table S2.

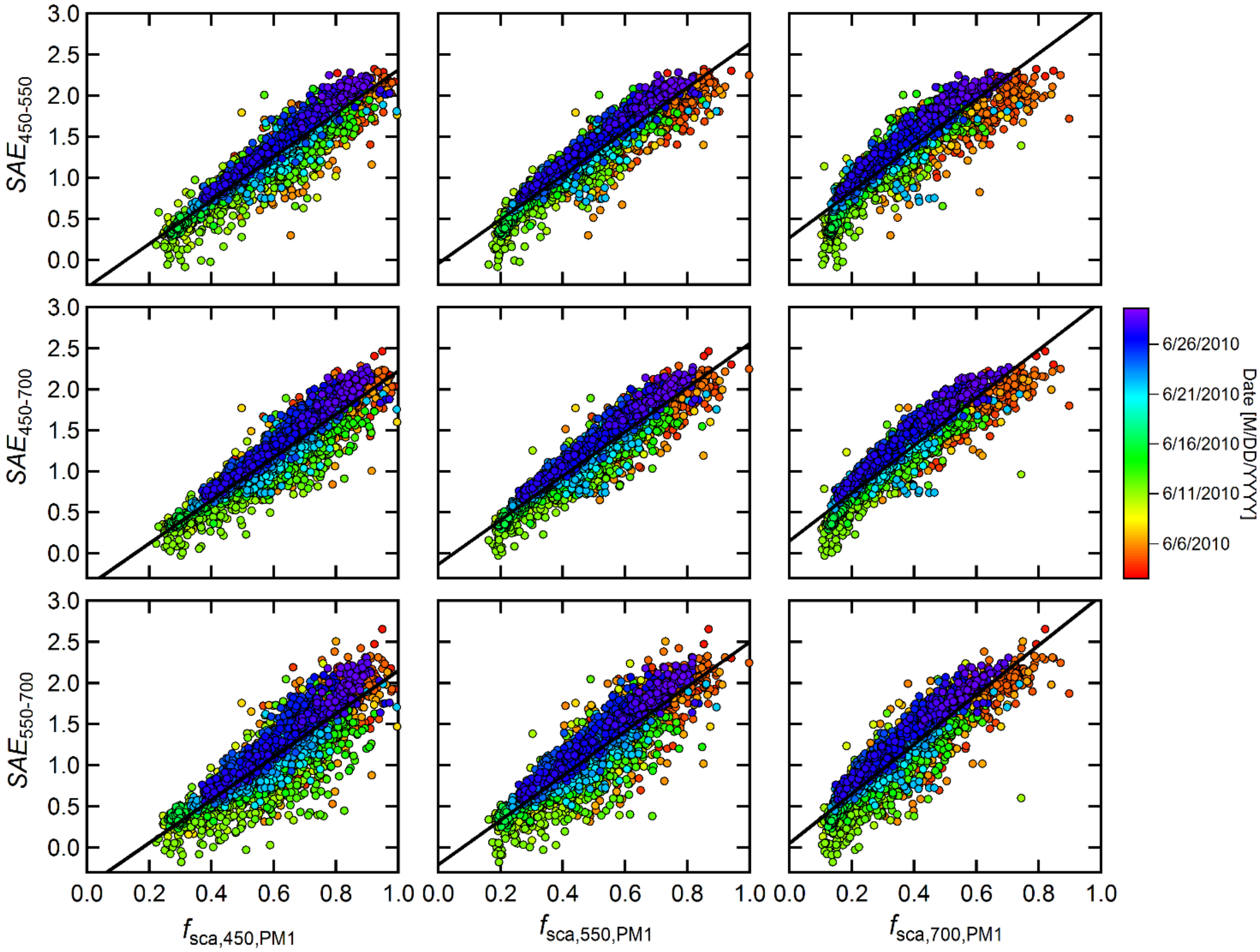

Figure S5. The relationship between the scattering Ångstrom exponent for PM_{10} for different wavelength pairs and the PM_1/PM_{10} scattering ratio ($f_{sca,PM1}$) at different wavelengths for the T1 site. The points are colored according to time during the campaign. Slope and intercept values from the linear fits (black lines) are reported in Table S2.

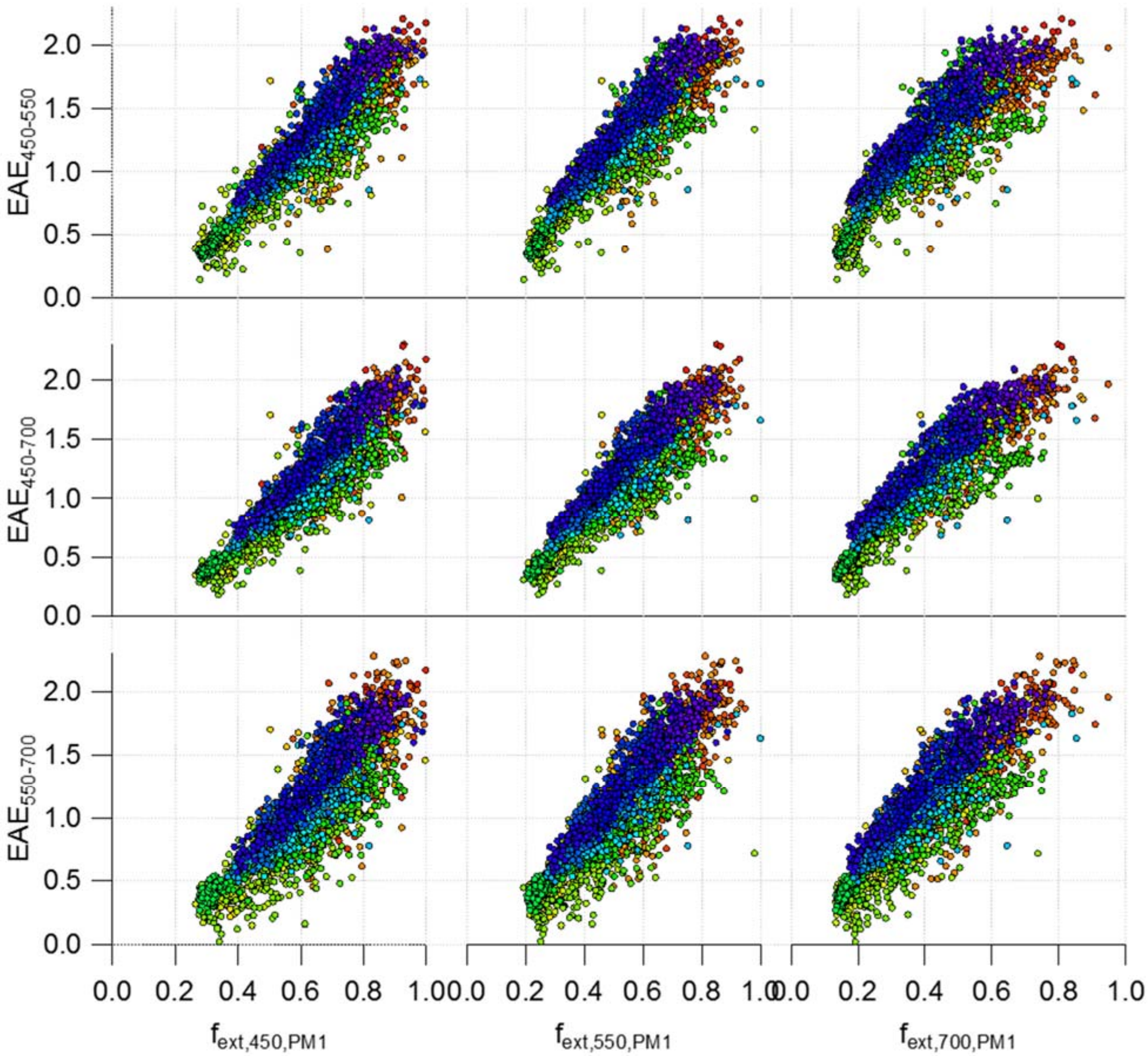

Figure S6. The relationship between the extinction Ångstrom exponent for PM_{10} for different wavelength pairs and the PM_1/PM_{10} extinction ratio ($f_{ext,PM1}$) at different wavelengths for the T0 site. The points are colored according to time during the campaign, as in Figure S4. The *EAE* values when $f_{ext,PM1} = 0.5$ are reported in Table S3.

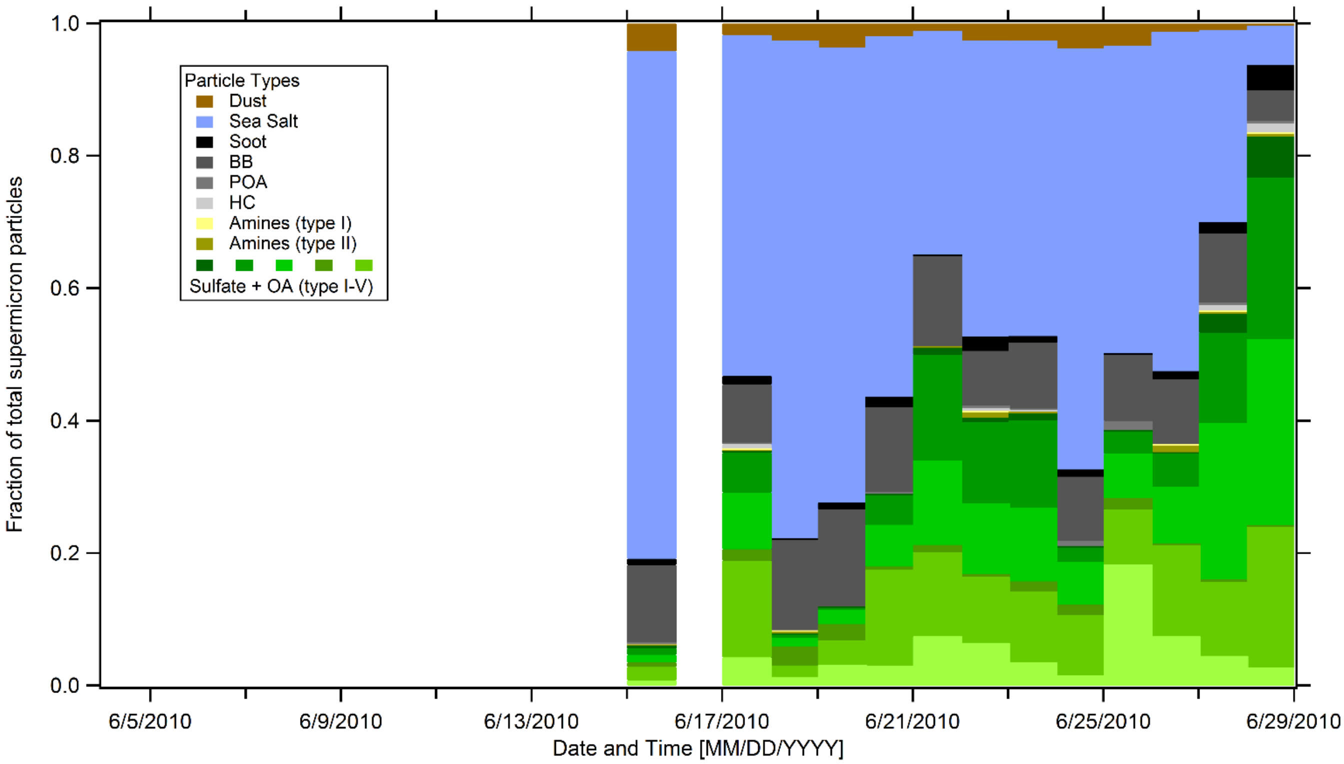

Figure S7. Fractional number abundance of supermicron particles (d_{va} > 1 micron) as measured by the SPLAT-II instrument at the T0 site. It should be noted that the upper-limit sampling range for SPLAT-II is around 2 microns, and thus supermicron particles that are larger than this are not characterized.

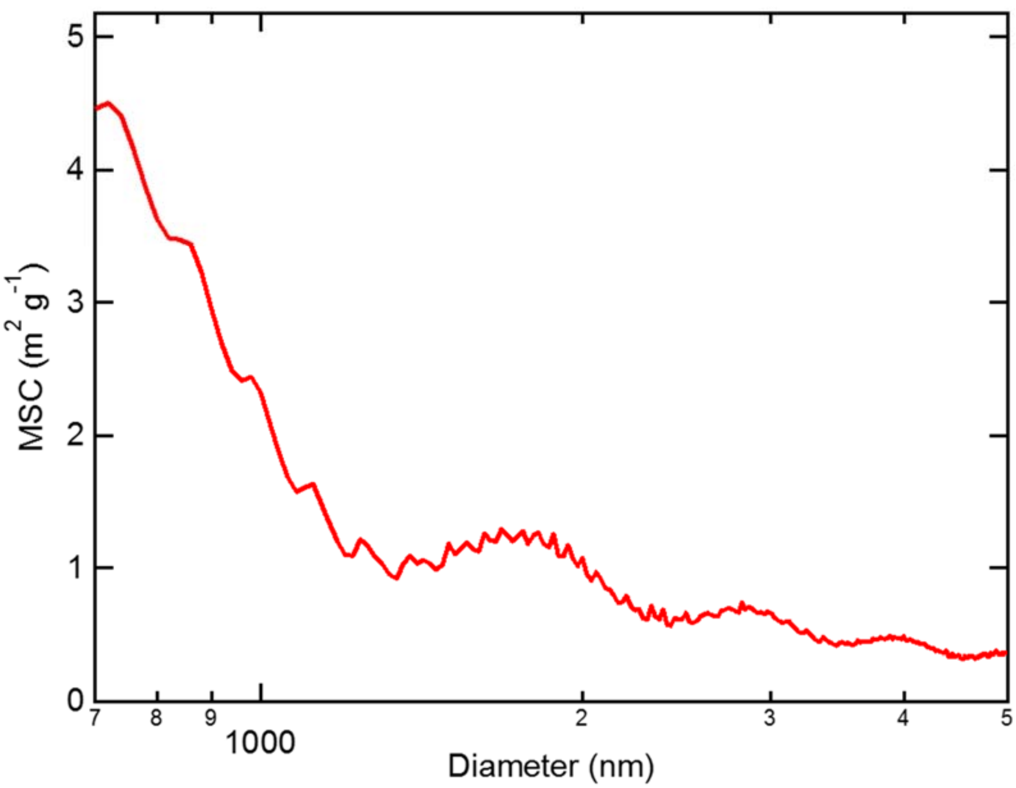

Figure S8. Calculated relationship between the mass scattering coefficient and mobility diameter for spherical particles with density = 2 g cm^{-3}. A complex refractive index of RI = 1.5 + 0.0*i* was used.

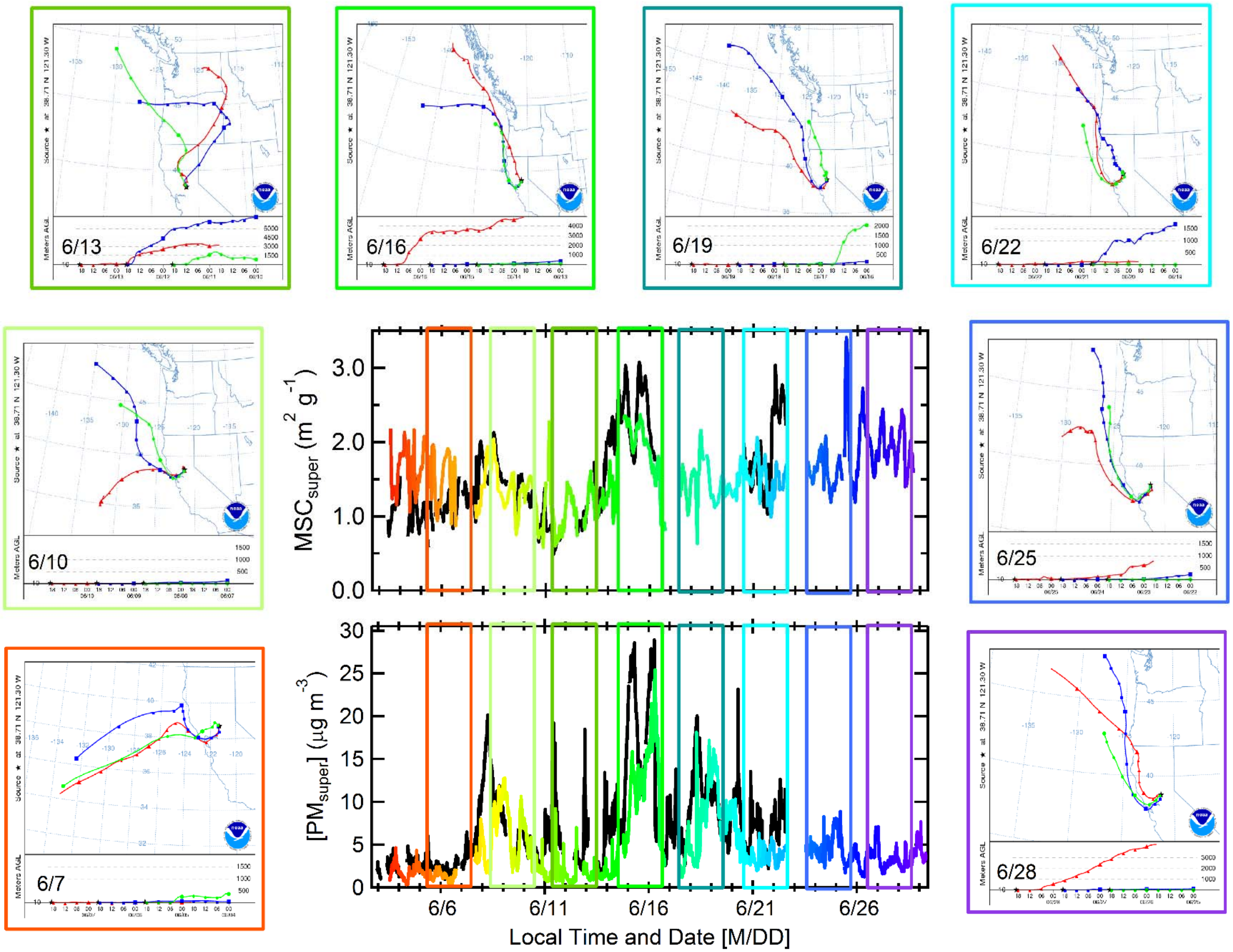

Figure S9. The central panels show time-series of the mass scattering coefficient and PM concentration for supermicron particles for both T0 (black lines) and T1 (colored lines). The outer panels show back trajectories calculated form HYSPLIT, using the NAM meteorological data, arriving at the T0 site at noon local time each day. Each outer panel shows three back trajectories that are separated by 24 hours (note that time goes backwards in these panels). The boxes around each outer panel correspond in color to the boxes shown in each of the central panels and provide a visual reference as to which trajectories correspond to which time period.

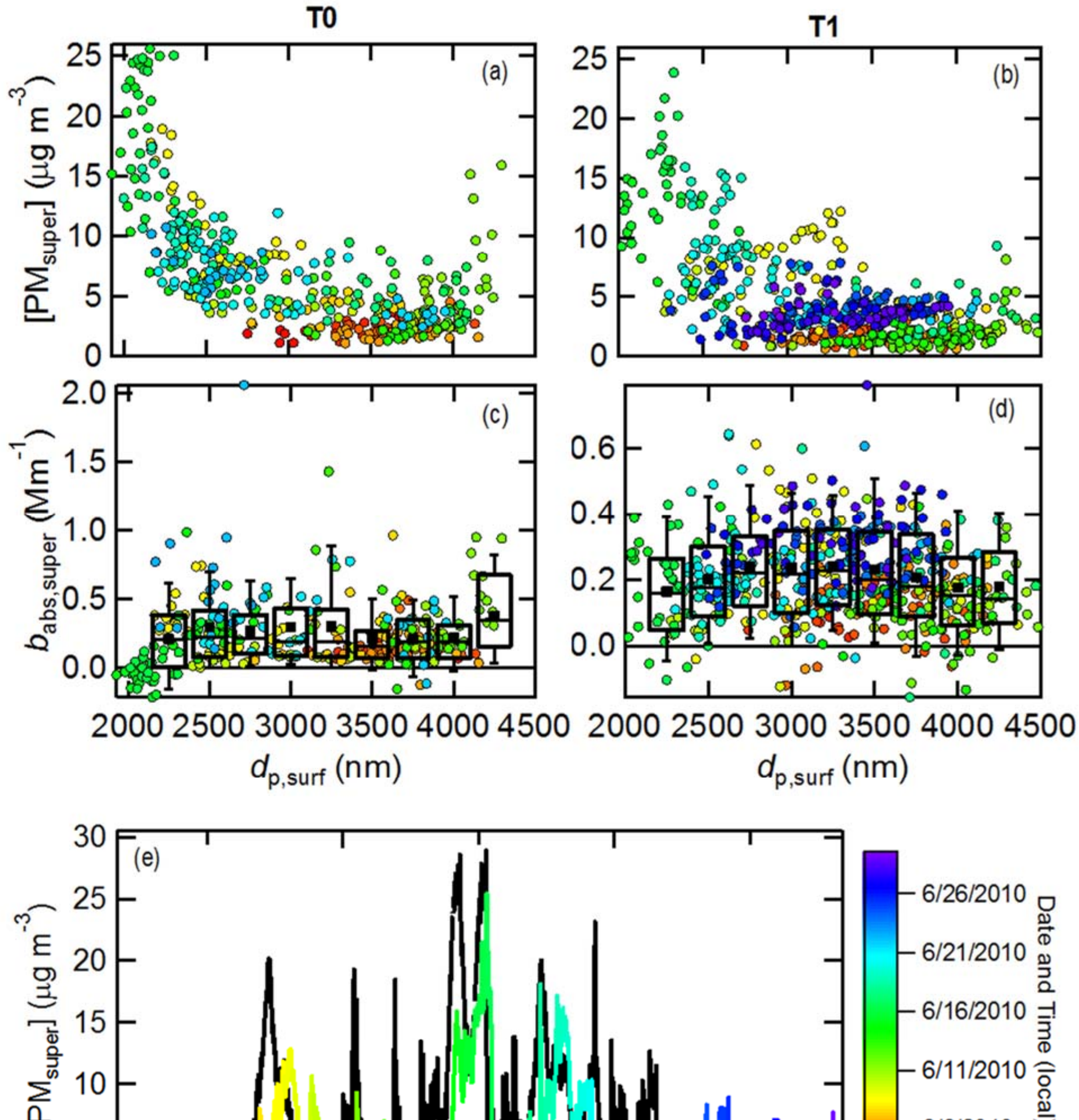

Figure S10. The relationship between the supermicron particle concentration (a,b) or the absolute supermicron absorption at 532 nm (c,d) and the surface-weighted median diameter of the supermicron mode. Observations from T0 are shown in (a) and (c) and from T1 in (b) and (d). For reference, the time series of [PM_{super}] is shown for both sites in panel (e), where T0 is shown in black and T1 in color. The points are colored according to date, as indicated in the color scale.

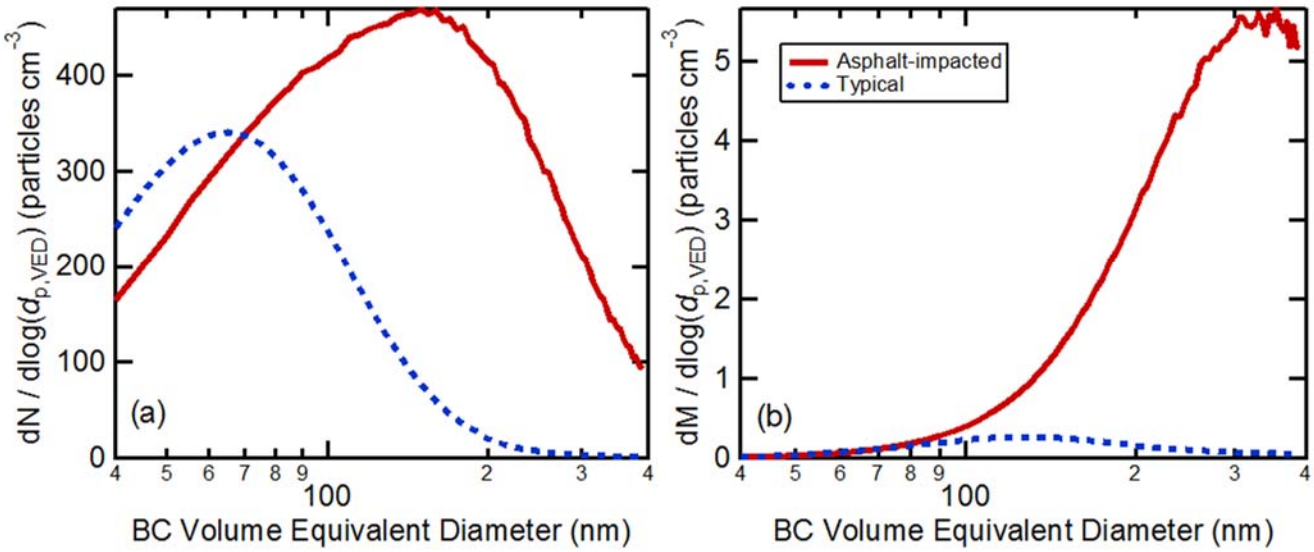

Figure S11. Refractory BC (a) number-weighted and (b) mass-weighted size distributions measured by the SP2 during the asphalt impacted period (22 June between 1:15 am and 2:30 am, local time) and during typical time periods. The typical size distribution is shown as a dashed blue line and the asphalt-impacted period as a red line.